



The Abdus Salam  
International Centre for Theoretical Physics



2218-1

**Mediterranean School on Nano-Physics**  
*held in Marrakech - MOROCCO*

*2 - 11 December 2010*

**Terahertz applications of carbon-based nanostructures**

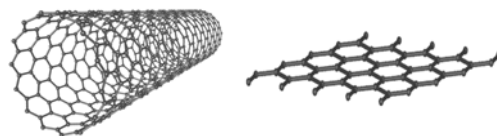
PORTNOI Mikhall E.  
*School of Physics University of Exeter*  
*Stocker Road EX4 4QL Exeter*  
*United Kingdom*



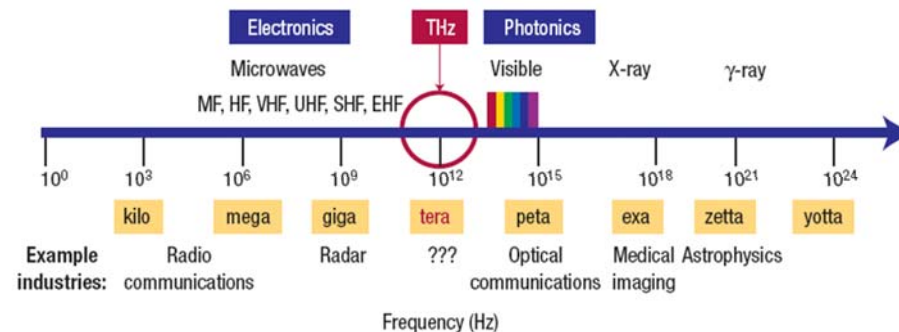
# Terahertz applications of carbon-based nanostructures

School of Physics  
University of Exeter  
United Kingdom

Mikhail E Portnoi



## Terahertz radiation and the 'THz gap'

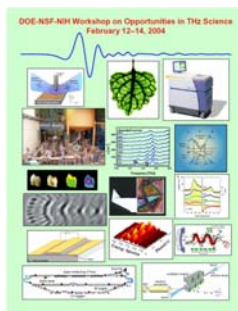


From B. Ferguson and X.-Ch. Zhang, *Nature Materials* 1, 26 (2002)

## Why is the THz range important?

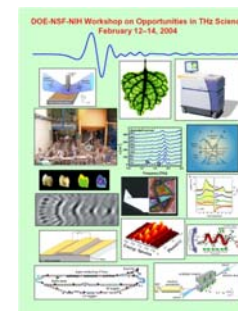
### Examples from the DOE-NSF-NIH Workshop Report, 2004

- Electrons in highly-excited atomic Rydberg states orbit at THz frequencies
- Small molecules rotate at THz frequencies
- Collisions between gas phase molecules at room temperature last about 1 ps
- Biologically-important collective modes of proteins vibrate at THz frequencies
- Frustrated rotations and collective modes cause polar liquids (such as water) to absorb at THz frequencies



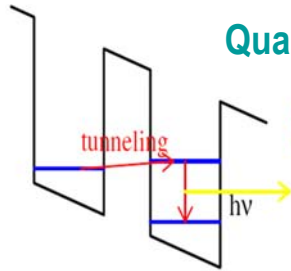
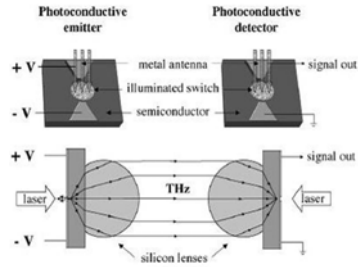
### More examples from the DOE-NSF-NIH Workshop Report

- Electrons in semiconductors and their nanostructures resonate at THz frequencies
- Superconducting energy gaps are found at THz frequencies
- Gaseous and solid-state plasmas oscillate at THz frequencies
- Matter at temperatures above 10 K emits black-body radiation at THz frequencies
- An electron in Intel's THz Transistor races under the gate in ~1 ps ...



**Transition region between photonics and electronics => unprecedented creativity in source development!**

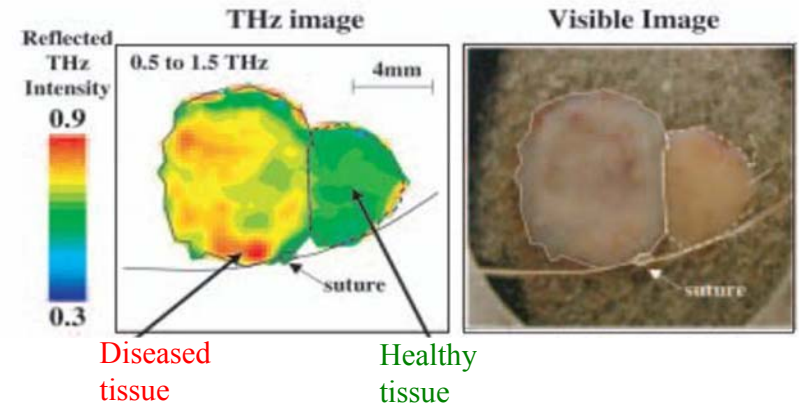
## TeraView scanner ~ \$500K



## Quantum cascade laser

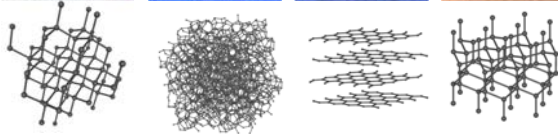
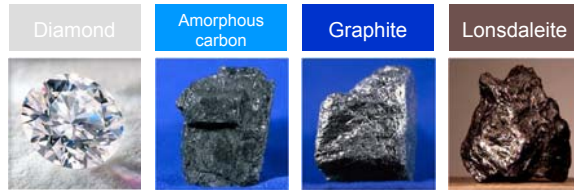
Kazarinov and Suris, 1971

*It took 23 years to achieve this laser!*

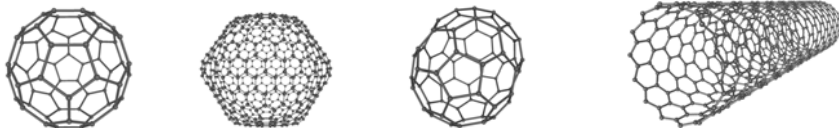


Images from TeraView Limited

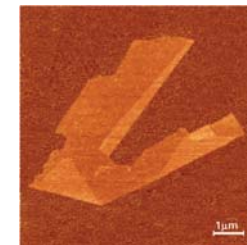
## Allotropes of Carbon



C60 (Buckminsterfullerene)	C540	C70	Carbon nanotube
----------------------------	------	-----	-----------------



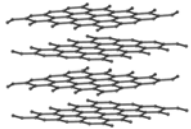
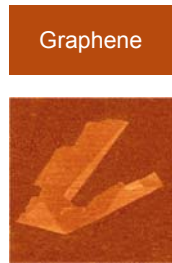
## Graphene



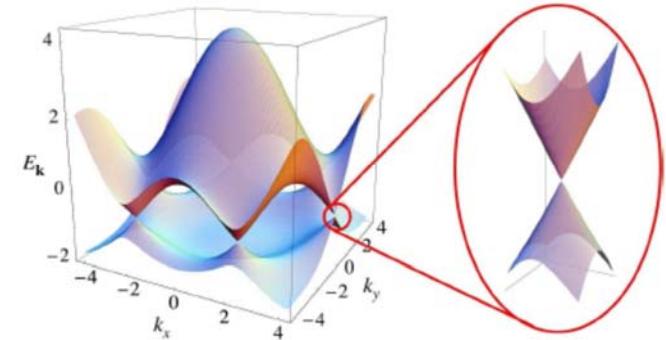
Atomic force microscopy image of a graphene flake.



# Graphite to Graphene



K.S. Novoselov et al., Science **306**, 666 (2004).

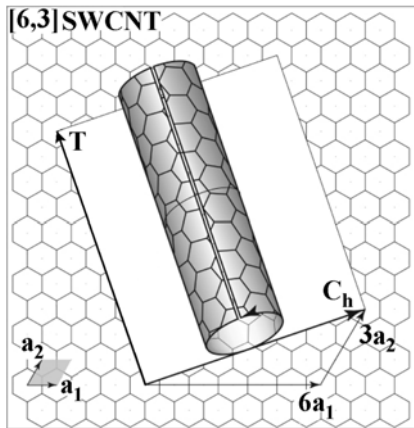


## Graphene dispersion.

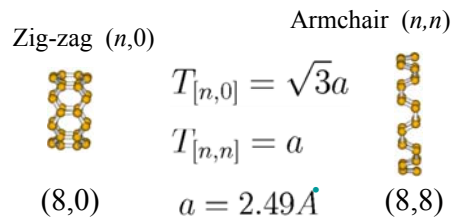
P.R. Wallace, *The band theory of graphite.*  
Phys. Rev. **71**, 622–634 (1947).

# Carbon nanotubes:

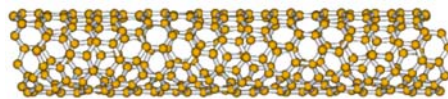
## Classification



### Achiral Nanotubes:



### Chiral Nanotubes:



$(n,m) :$

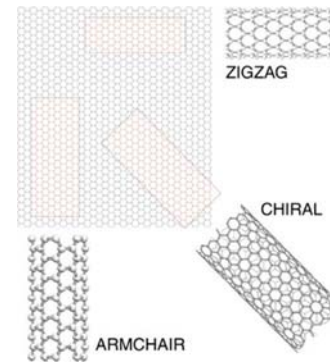
$$\mathbf{C}_h = n\mathbf{a}_1 + m\mathbf{a}_2$$

$$|\mathbf{T}| = \sqrt{3} |\mathbf{C}_h| / d_R$$

$$d_R = \text{gcd} [2n + m, 2m + n]$$

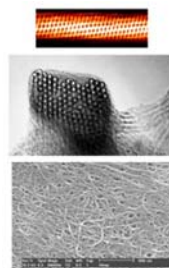
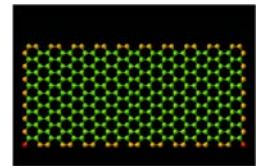
$(8,1)$

$$T_{[8,1]} = 14.8a = 36.8\text{\AA}$$

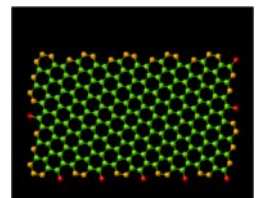


[from www.seas.upenn.edu]

## Ideal and real CNTs



CNTs produced by laser ablation of a graphite target containing metal catalyst additives.

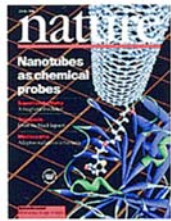


[from  
www.surf.nuqe.nagoya-u.ac.jp  
and www.photon.t.u-tokyo.ac.jp]



# Carbon nanotubes:

## Applications



Chemical/Biological



Electronic



Mechanical

THz?

# Previous proposals

Nanoklystron utilizing efficient high-field electron emission from nanotubes:

D. Dragoman and M. Dragoman, *Progr. Quant. Electron.* **28**, 1 (2004);  
 H.M. Manohara *et.al.*, *J. Vac. Sci. Technol. B* **23**, 157 (2005);  
 Aldo Di Carlo *et.al.*, *Proc. SPIE* 632808 (2006).

Devices based on negative differential conductivity in large-diameter semiconducting CNTs:

A.S. Maksimenko and G.Ya. Slepyan, *Phys. Rev. Lett.* **84**, 362 (2000);  
 G. Pennington and N. Goldsman, *Phys. Rev. B* **68**, 045426 (2003).

High-frequency resonant-tunneling and Schottky diodes:

A.A. Odintsov, *Phys. Rev. Lett.* **85**, 150 (2000);  
 F. Leonard and J. Tersoff, *Phys. Rev. Lett.* **85**, 4767 (2000);  
 D. Dragoman and M. Dragoman, *Physica E* **24**, 282 (2004).

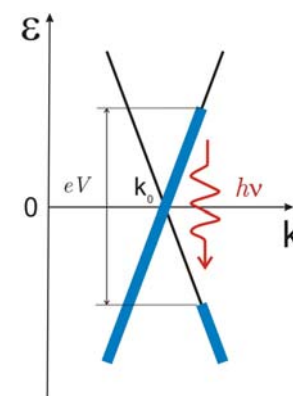
THz frequency multipliers, amplifiers and antennas:

G.Ya. Slepyan *et. al.*, *Phys. Rev. A* **60**, 777 (1999); *ibid.* **63**, 53808 (2000);  
 D. Dragoman and M. Dragoman, *Physica E* **25**, 492 (2005);  
 G.Ya. Slepyan *et.al.*, *Phys. Rev. B* **73**, 195416 (2006); *Proc. SPIE* 632806 (2006).

## OUTLINE

- Introduction
- Generation of THz radiation by hot electrons in quasi-metallic CNTs
- Chiral CNTs as frequency multipliers
- Armchair CNTs in a magnetic field as tunable THz sources and detectors
- Polarization-sensitive THz detectors based on graphene p-n junctions

## Generation of THz radiation by hot carriers in quasi-metallic CNTs



$$\varepsilon(k) = \pm v_F |k - k_0|$$

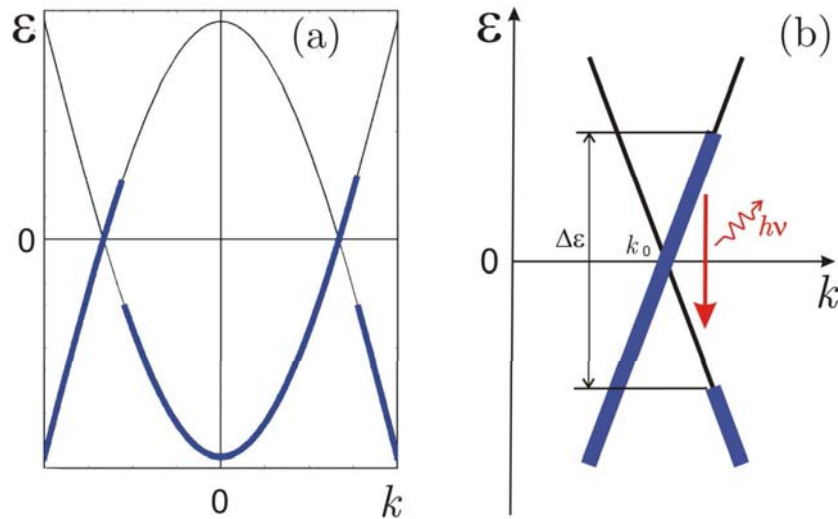
$$L < l_{ac} \quad (\text{acoustic scattering mean free path, approximately } 2 \mu\text{m})$$

$$eV < \hbar\Omega$$

(energy of zone-boundary / optical phonons of around 160 / 200 meV)

The scheme of THz photon generation by hot carriers in quasi-metallic CNTs in the ballistic regime.

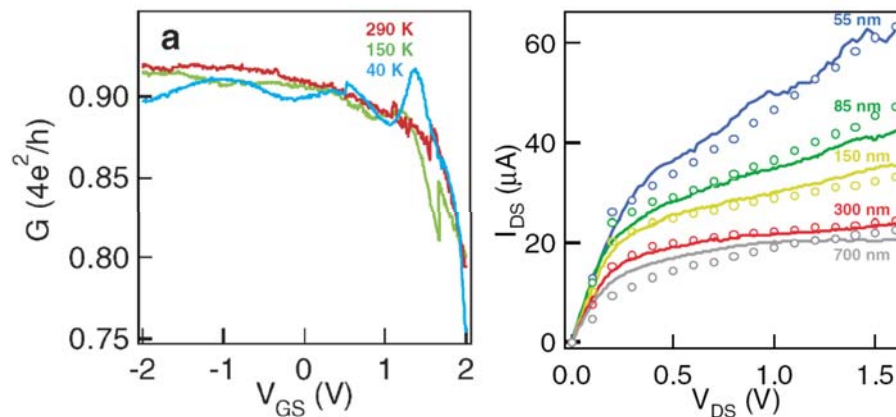
$$f_e(k) = \begin{cases} 1, & 0 < k - k_0 < \Delta\varepsilon/2\hbar v_F \\ 0, & k - k_0 > \Delta\varepsilon/2\hbar v_F \end{cases}$$



## Ballistic transport and phonon scattering: Key publications

- T. Ando, t. Nakanishi, and R. Saito, J. Phys. Soc. Jpn. **67**, 1704 (1997)
- Z. Yao, C.L. Kane, and C. Dekker, Phys. Rev. Lett. **84**, 2941 (2000)
- A. Javey *et. al.*, Phys. Rev. Lett. **92**, 106804 (2005)
- J.-Y. Park *et. al.*, Nano Lett. **4**, 517 (2004)
- M. Freitag *et. al.*, Nano Lett **4**, 1063 (2004)
- V.Perebeinos, J.Tersoff, and P. Avouris, Phys.Rev.Lett. **94**, 86802 (2004)
- M.P.Anantram and F.Léonard, Rep. Prog. Phys. **69**, 507 (2006)

## Ballistic transport and phonon scattering



From A. Javey *et. al.*, Phys. Rev. Lett. **92**, 106804 (2004)

## Optical transitions in CNTs (recent papers only)

- I. Milošević *et. al.*, Phys. Rev. B **67**, 165418 (2003)
- J. Jiang *et. al.*, Carbon **42**, 3169 (2004)
- A. Grüneis *et. al.*, Phys. Rev. B **67**, 165402 (2003)
- V.N. Popov and L. Henrard, Phys. Rev. B **70**, 115407 (2004)
- R. Saito *et. al.*, Appl. Phys. A **78**, 1099 (2004)
- S.V. Goupalov, Phys. Rev. B **72**, 195403 (2005)
- Y. Oyama, Carbon **44**, 873 (2006)

**Optical transitions between the lowest conduction subband and the top valence subband of a true metallic (armchair) CNT are forbidden!**

## Quasi-metallic nanotubes

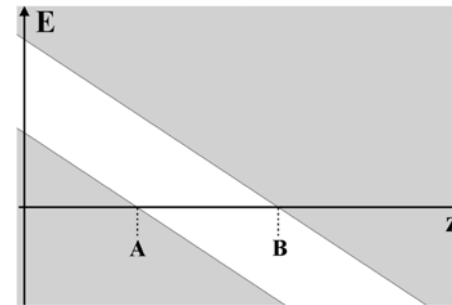
are  $(n,m)$  SWNTs with  $n-m=3p$ , where  $p$  is a non-zero integer.

Their bandgap is given by 
$$\varepsilon_g = \frac{\hbar v_F a_{C-C} \cos 3\theta}{8R^2},$$

where  $a_{C-C} = 1.42 \text{ \AA}$  is the nearest-neighbor distance between two carbon atoms,  $R$  is the CNT radius, and  $\theta = \arctan[\sqrt{3}m/(2n+m)]$  is a chiral angle.

[See, e.g., C.L. Kane and E.J. Mele, Phys. Rev. Lett. 78, 1932 (1997)]

## Zener tunneling



For the energy spectrum near the gap given by

$$\varepsilon = \pm \sqrt{\varepsilon_g^2 / 4 + \hbar^2 v_F^2 k^2}$$

the tunneling exponent is

$$\exp\left(-\frac{\pi}{4} \frac{\varepsilon_g^2}{eE\hbar v_F}\right)$$

For example, for a zig-zag (30,0) CNT the gap is about 6meV and the Zener breakdown occurs for the electric field of about 0.1 V/ $\mu$ m.

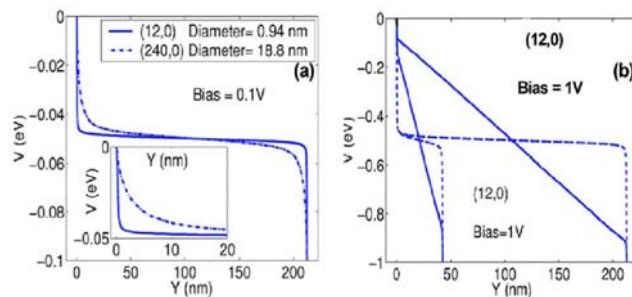


**Figure 17.** Electrostatic potential versus length along nanotube axis. (a) Low bias potential versus position for (12,0) and (240,0) nanotubes, which have diameters of 0.94 nm and 18.8 nm, respectively. The applied bias is 100 mV. The screening for the large-diameter nanotube is significantly poorer. The inset magnifies the potential close to the nanotube-contact interface, showing that in contrast to the nanotube bulk the electric field is smaller at the edges when the diameter is larger (density of states is smaller). The nanotube length is 213 nm. (b) The potential as a function of position is shown for (12,0) nanotubes of lengths 42.6 and 213 nm in the presence of scattering (—). The potential profile in the ballistic limit (- - -) is shown for comparison.

From M.P. Anantram and F. Léonard, Rep. Prog. Phys. 69, 507 (2006)

## Dipole optical transitions in CNTs

I. Milošević *et al.*, Phys. Rev. B 67, 165418 (2003)

A. Grüneis *et al.*, Phys. Rev. B 67, 165402 (2003)

J. Jiang *et al.*, Carbon 42, 3169 (2004)

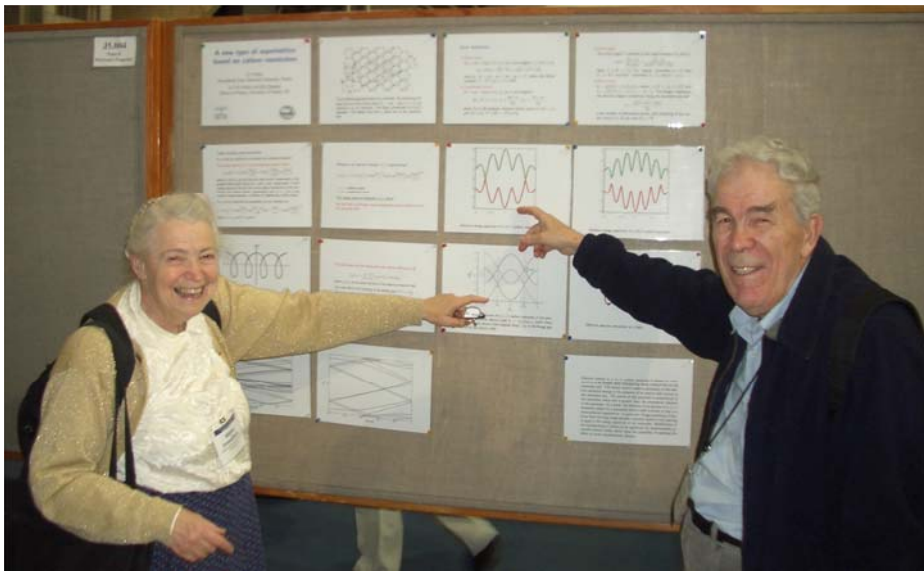
V.N. Popov and L. Henrard, Phys. Rev. B, 70, 115407 (2004)

R. Saito *et al.*, Appl. Phys. A 78, 1099 (2004)

S.V. Goupalov, Phys. Rev. B 72, 195403 (2005)

Y. Oyama, Carbon 44, 873 (2006)

**Nearest-neighbor orthogonal  $\pi$ -electron tight-binding model**



M.S. Dresselhaus & G. Dresselhaus, Fort Collins, Arizona, August 2004

## Dipole optical transitions polarized along the CNT axis

The spectral density of spontaneous emission:

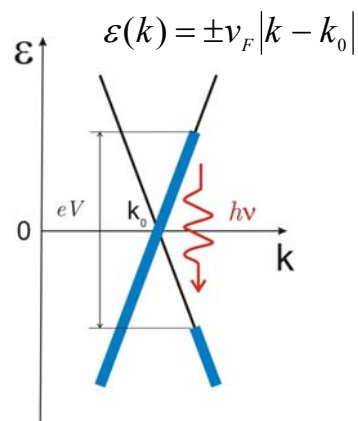
$$I_\nu = \frac{8\pi e^2 \nu}{3c^3} \sum_{i,f} f_e(k_i) f_h(k_f) |\langle \Psi_f | \hat{v}_z | \Psi_i \rangle|^2 \delta(\varepsilon_i - \varepsilon_f - h\nu).$$

Using  $v_z = i/\hbar[H, r]$  and the properties of the tight-binding Hamiltonian we get for the transitions between the lowest conduction and the highest valence subband of a (3p,0) zigzag CNT:

$$\langle \Psi_f | \hat{v}_z | \Psi_i \rangle = \frac{a_{C-C} \omega_{if}}{8} \delta_{k_f, k_i}, \quad \text{where } \hbar\omega_{if} = \varepsilon_i - \varepsilon_f. \quad \text{Finally,}$$

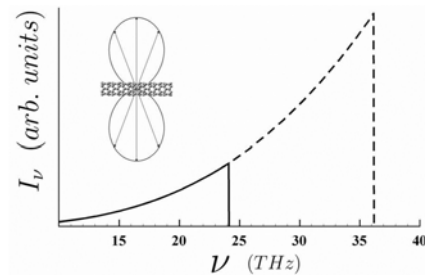
$$I_\nu = L f_e(\pi\nu/v_F) f_h(\pi\nu/v_F) \frac{\pi^2 e^2 a_{C-C}^2 \nu^3}{6c^3 \hbar v_F}.$$

A similar expression (corrected by a numerical factor depending on a chiral angle  $\theta$ ) is valid for any quasi-metallic CNT.



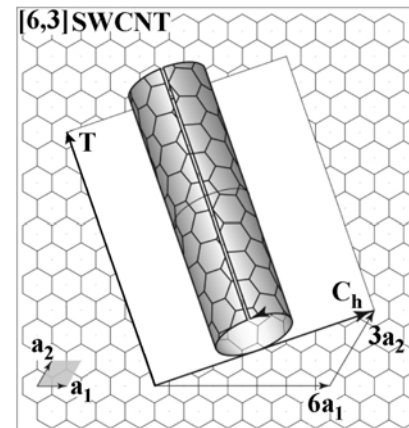
The scheme of THz photon generation by hot carriers in quasi-metallic CNTs in the ballistic regime.

[O.V.Kibis, M.Rosenau da Costa, M.E.Portnoi, Nano Lett. 7, 3414 (2007)]





The spectral density of spontaneous emission as a function of frequency for two values of applied voltage: solid line for  $V=0.1V$ ; dashed line for  $V=0.15V$ . The inset shows the directional radiation pattern of the THz emission with respect to the nanotube axis.

## Chiral CNTs as frequency multipliers

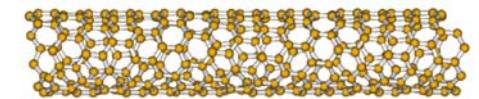


$$(n,m) : \begin{aligned} \mathbf{C}_h &= n\mathbf{a}_1 + m\mathbf{a}_2 \\ |\mathbf{T}| &= \sqrt{3} |\mathbf{C}_h| / d_R \\ d_R &= \text{gcd}[2n+m, 2m+n] \end{aligned}$$

Achiral nanotubes:

Zig-zag $(n,0)$		Armchair $(n,n)$
	$T_{[n,0]} = \sqrt{3}a$	
	$T_{[n,n]} = a$	
$(8,0)$	$a = 2.49\text{\AA}$	$(8,8)$

Chiral nanotubes:

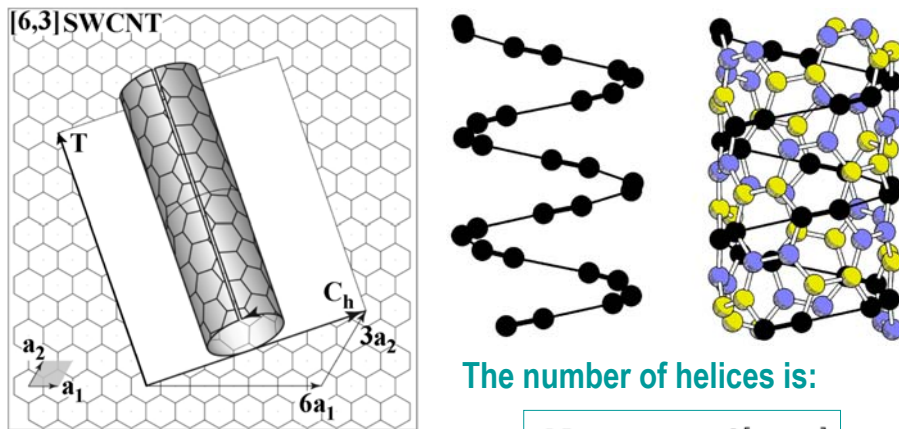


$$(8,1) \quad T_{[8,1]} = 14.8a = 36.8\text{\AA}$$



## Helical symmetries in chiral CNTs

C.T. White, D.H. Hoberstons and J.W. Mintmire, PRB 47, 5485 (1993).

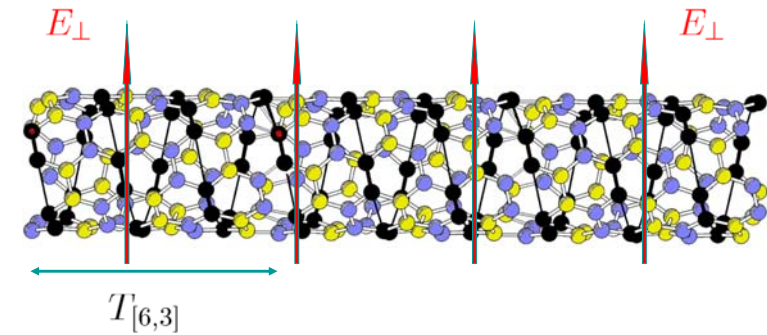


The number of helices is:

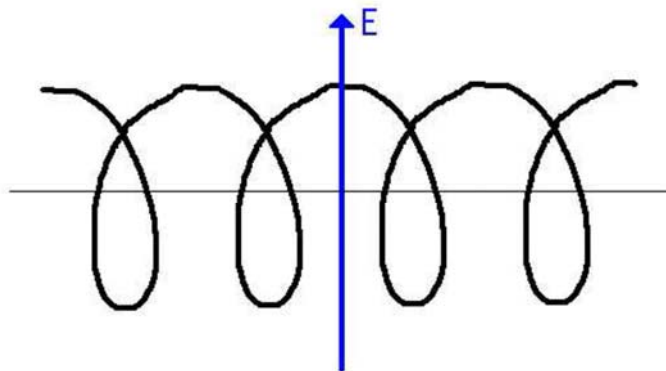
$$N_{Helix} = \text{gcd}[n, m]$$

## Superlattice properties of chiral CNTs in a transverse Electric Field

O.V. Kibis, D.G.W. Parfitt and M.E. Portnoi, PRB 71, 35411 (2005).

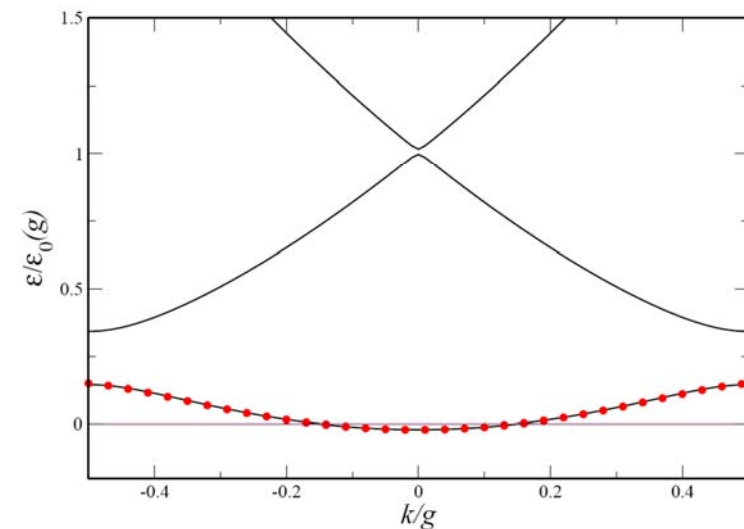


The helical symmetry provides an idea of the origin of the superlattice properties.



Helix in a transverse electric field

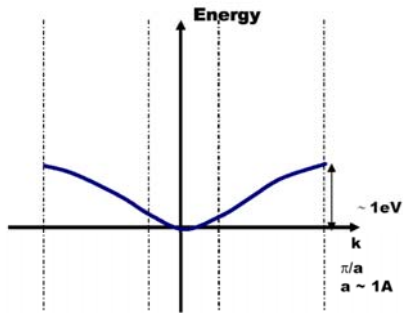
The potential energy of an electron on a helix subject to a transverse electric field takes the form  $U = eER \cos(2\pi s/l_0)$ , where  $e$  is the electron charge,  $E$  is the electric field strength,  $R$  is the radius of the helix,  $l_0$  is the length of the single coil and  $s$  is the electron coordinate along the spiral line.



Electron energy spectrum of a nanohelix in the presence of a transverse electric field  $E = 0.2\varepsilon_0(g)/(eR)$ : solid lines – result of numerical diagonalisation of a  $7 \times 7$  matrix; red circles – simple analytic approximation.

## Bloch oscillations (BOs) and criterion of their existence

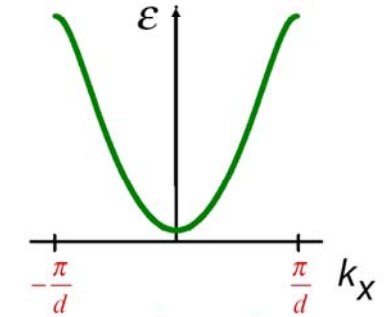
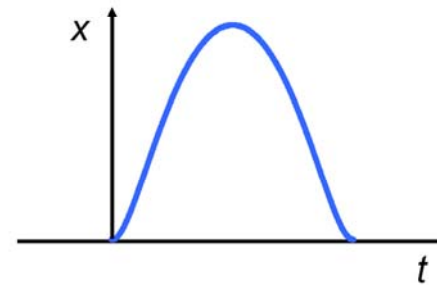
**Bulk Semiconductor**



$$\hbar \frac{dk}{dt} = eE_{dc} \quad \text{Bloch, 1928}$$

Courtesy of Kirill Alekseev

A particle which is accelerated through k-space performs an oscillation in real space.



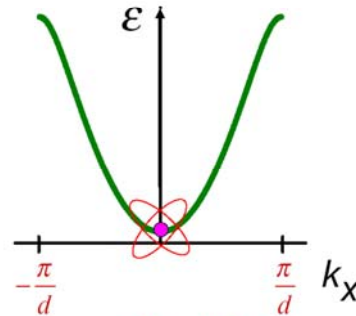
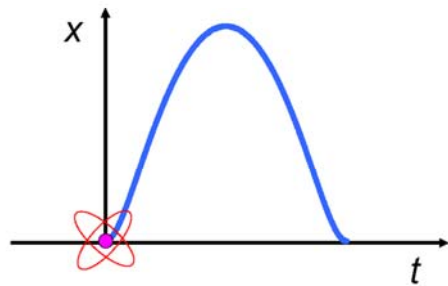
This is known as a Bloch oscillation.

$$V = \frac{dx}{dt} = \frac{1}{\hbar} \frac{d\varepsilon}{dk_x}$$

$$\hbar \frac{dk_x}{dt} = eE_{dc}$$

© Kirill Alekseev

A particle which is accelerated through k-space performs an oscillation in real space.



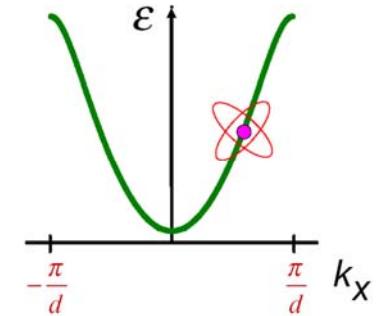
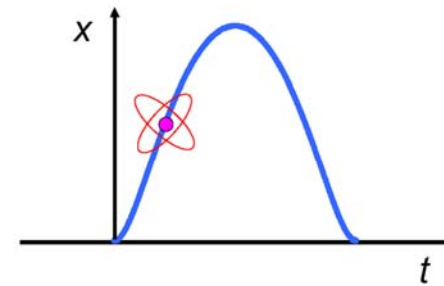
This is known as a Bloch oscillation.

$$V = \frac{dx}{dt} = \frac{1}{\hbar} \frac{d\varepsilon}{dk_x}$$

$$\hbar \frac{dk_x}{dt} = eE_{dc}$$

© Kirill Alekseev

A particle which is accelerated through k-space performs an oscillation in real space.



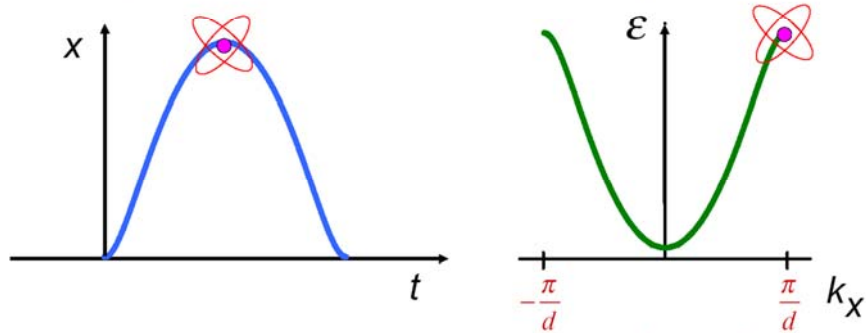
This is known as a Bloch oscillation.

$$V = \frac{dx}{dt} = \frac{1}{\hbar} \frac{d\varepsilon}{dk_x}$$

$$\hbar \frac{dk_x}{dt} = eE_{dc}$$

© Kirill Alekseev

A particle which is accelerated through k-space performs an oscillation in real space.



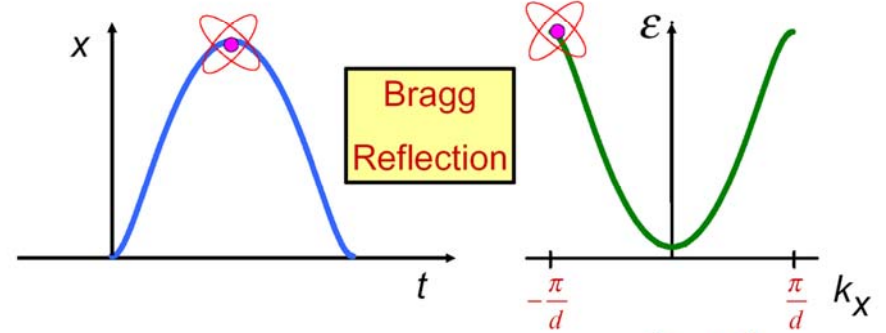
This is known as a Bloch oscillation.

© Kirill Alekseev

$$V = \frac{dx}{dt} = \frac{1}{\hbar} \frac{d\varepsilon}{dk_x}$$

$$\hbar \frac{dk_x}{dt} = eE_{dc}$$

A particle which is accelerated through k-space performs an oscillation in real space.



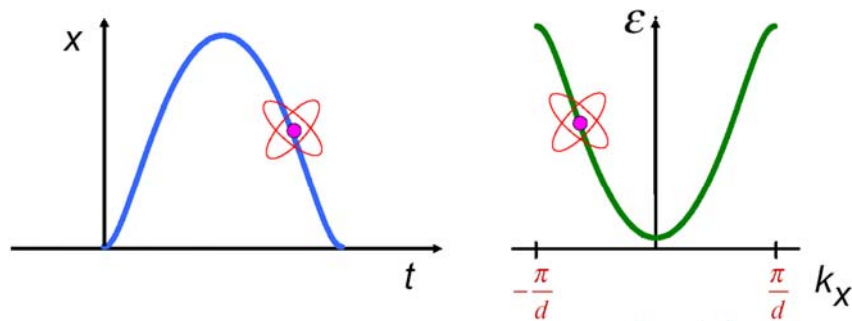
This is known as a Bloch oscillation.

© Kirill Alekseev

$$V = \frac{dx}{dt} = \frac{1}{\hbar} \frac{d\varepsilon}{dk_x}$$

$$\hbar \frac{dk_x}{dt} = eE_{dc}$$

A particle which is accelerated through k-space performs an oscillation in real space.



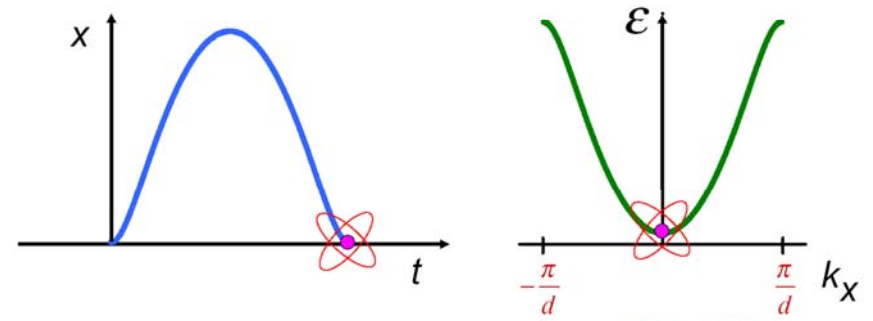
This is known as a Bloch oscillation.

© Kirill Alekseev

$$V = \frac{dx}{dt} = \frac{1}{\hbar} \frac{d\varepsilon}{dk_x}$$

$$\hbar \frac{dk_x}{dt} = eE_{dc}$$

A particle which is accelerated through k-space performs an oscillation in real space.



This is known as a Bloch oscillation.

© Kirill Alekseev

$$V = \frac{dx}{dt} = \frac{1}{\hbar} \frac{d\varepsilon}{dk_x}$$

$$\hbar \frac{dk_x}{dt} = eE_{dc}$$



Time period of BOs:

$$\tau_B = \frac{h}{eaE_{dc}}$$

Frequency of BOs:

$$\omega_B = \frac{eaE_{dc}}{\hbar}$$

### Criterion of BOs existence

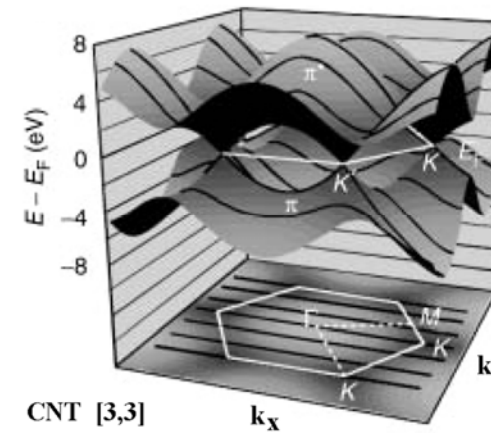
high fields  
and/or  
long scattering times

$$\tau \gg \tau_B$$

$$\omega_B \tau \geq 1$$

© Kirill Alekseev

### Zone-folding method in a single $\pi$ -band tight binding model



The allowed values of  $k$  are:

$$\mathbf{k} = k_{\parallel} \hat{\mathbf{T}} + k_{\perp} \hat{\mathbf{C}}_h,$$

with

$$-\pi/T < k_{\parallel} \leq \pi/T,$$

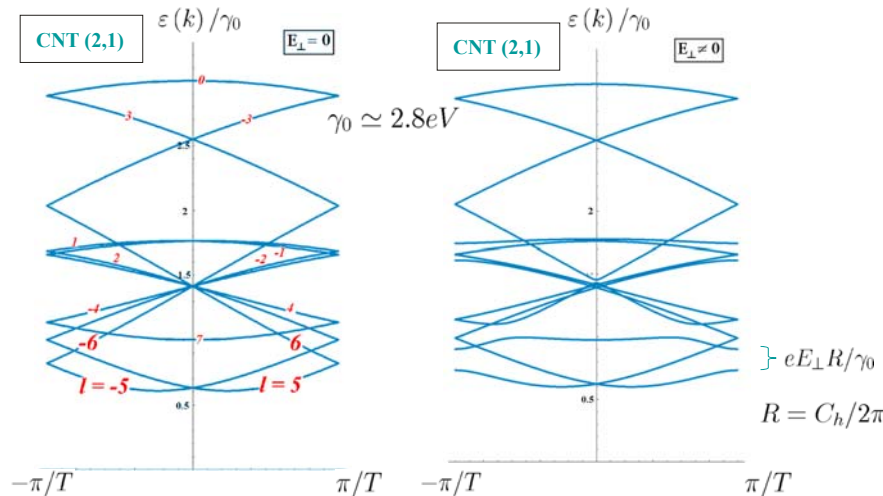
where

$$k_{\perp} = \frac{2\pi}{C_h} l,$$

$$l = -N/2 + 1, \dots, 0, 1, \dots, N/2.$$

$N$  is the number of hexagons in the CNT unit cell.

### Transverse electric field opens gaps in the CNT energy spectrum

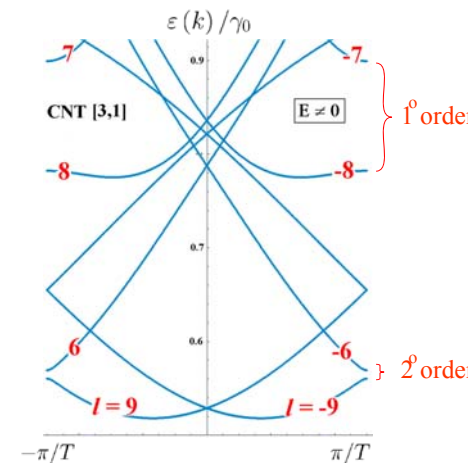


First order gaps between the subbands such that:  $l' = l \pm 1$

For the lowest band and other chiral nanotubes there are only higher

order gaps:  $\Delta_{Gap}^{1^a B} \propto \left( \frac{eE_{\perp} C_h}{2\pi\gamma_0} \right)^n$ .

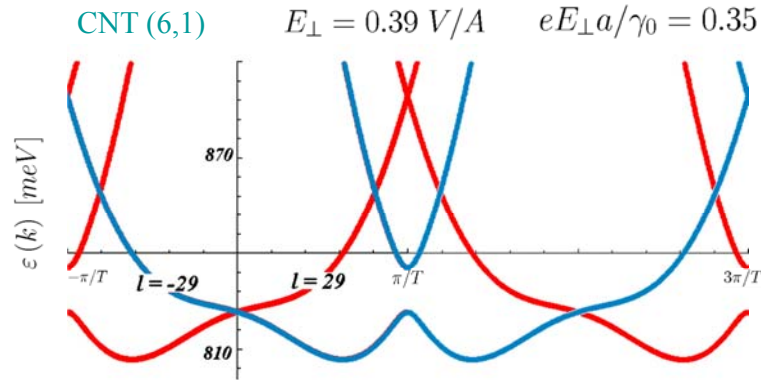
For the  $(n,1)$  family we have:



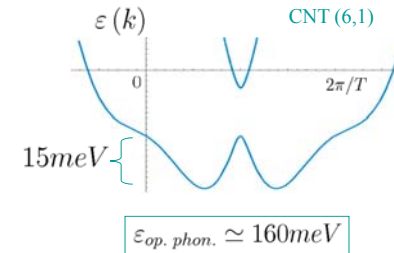
CNT	Gap Order	$T/a$
(2,1)	1	4.6
(3,1)	2	6.3
(4,1)	2	2.6
(5,1)	2	9.6
(6,1)	3	11.4
(7,1)	3	4.4
(8,1)	3	14.8
(9,1)	4	16.5
(10,1)	4	6.1



## Repeated-zone scheme



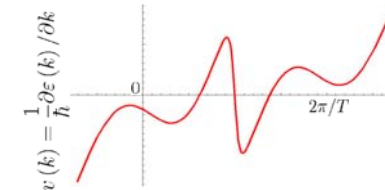
## Response to a DC Parallel Electric Field



In the semiclassical description:

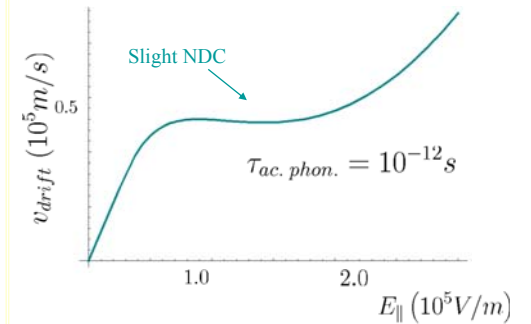
$$v_T(t) = v_1(t) + v_2(t),$$

$$v_i(t) = v_i(k_i(t)) = v\left(k_{0,i} + \frac{eE_{\parallel}}{\hbar}t\right).$$

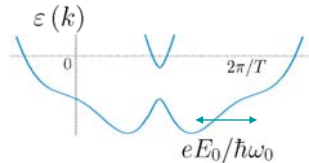


For the drift velocity (Esaki-Tsu):

$$v_{drift} = \int_0^{\infty} e^{-t/\tau} \frac{d}{dt} v_T(t) dt.$$



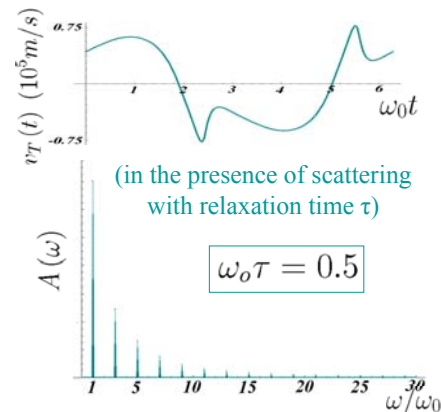
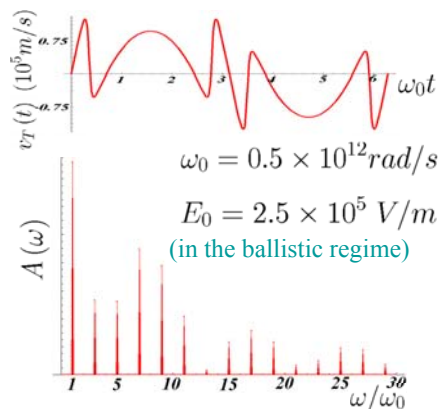
## Response to an AC parallel electric field



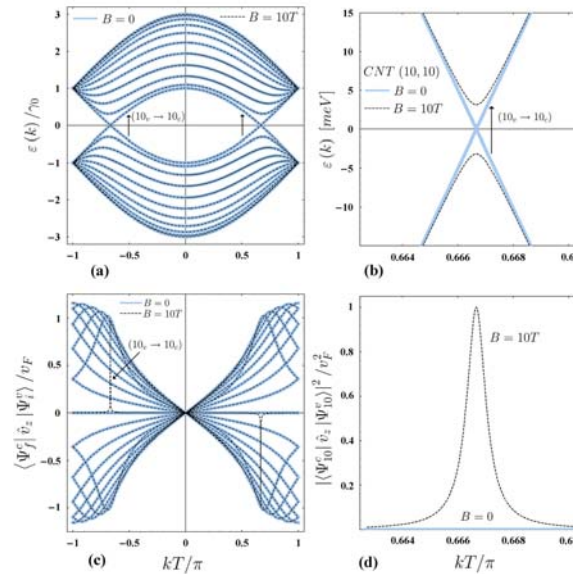
Applying an AC field:

$$E_{\parallel}(t) = E_0 \sin[\omega_0 t]$$

$$k(t) = k_0 + \frac{eE_0}{\hbar\omega_0} \sin(\omega_0 t).$$



## Armchair CNT in a magnetic field



Energy spectra and matrix elements of optical transitions polarized along the nanotube axis for a (10,10) CNT in a magnetic field  $B=10\text{T}$  along the nanotube axis and without the field.

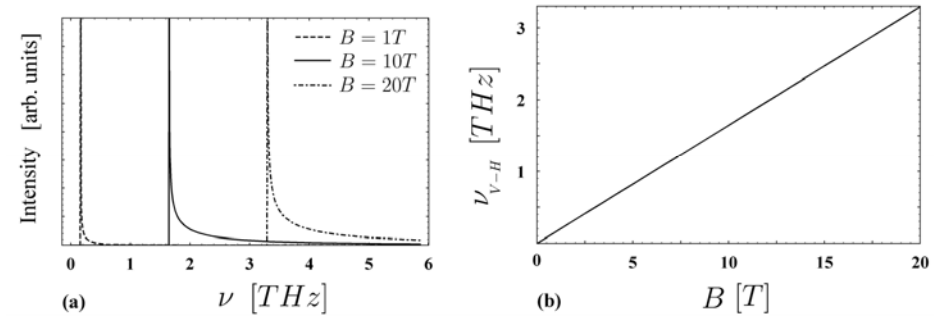
### Magnetic-field induced gap in an armchair (n,n) CNT:

$$\varepsilon_g = 2\gamma_0 \left| \sin\left(\frac{f}{n}\pi\right) \right|, \text{ where } f = \Phi/\Phi_0.$$

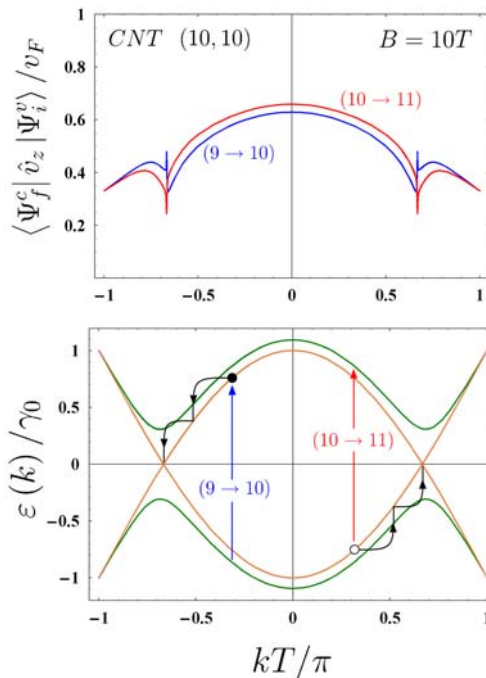
### Matrix element of velocity at the band edge:

$$\left| \langle \Psi_C | \hat{v}_z | \Psi_V \rangle \right| = v_F \frac{2}{\sqrt{3}} \left[ 1 - \frac{1}{4} \cos^2\left(\frac{f}{n}\pi\right) \right]^{1/2} \approx v_F$$

**Absorption intensity:**  $I(\varepsilon) \propto \frac{1}{\varepsilon^2} \frac{\varepsilon_g^{5/2}}{\sqrt{\varepsilon - \varepsilon_g}} \theta(\varepsilon - \varepsilon_g).$



- (a) Absorption intensity (taking into account the van-Hove singularity in the reduced density of states) for several magnetic field values.
- (b) The magnetic field dependence of the peak frequency for a (10,10) CNT.



The scheme for creating inversion of population in tunable THz emitters based on armchair CNTs in a magnetic field.

cond-mat/0608596;  
Proc. SPIE 632805 (2006);  
Superlattices and  
Microstructures (2007)

## THz applications of graphene

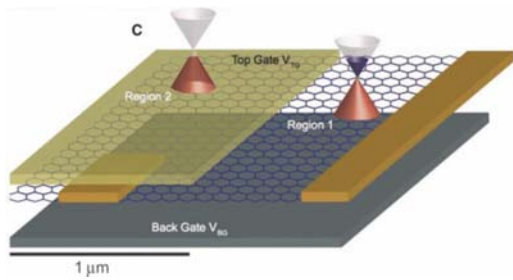
### Graphene as a THz emitter

Highly-efficient frequency multiplication due to non-parabolic electronic spectrum [S.A. Mikhailov, EPL **79**, 27002 (2007); Review – JPCM **20**, 384204(2008)]

### Graphene as a THz detector

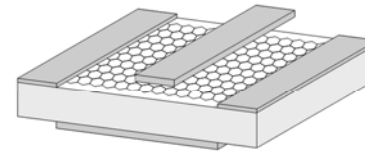
- Zero-gap semiconductor => THz absorption
- Gate control of the Fermi level position => tuneable low-frequency limit via the Moss-Burstein effect
- Momentum alignment of photoexcited carriers => polarisation sensitivity (for p-n junction structures)

# Klein tunneling and Graphene p-n junctions

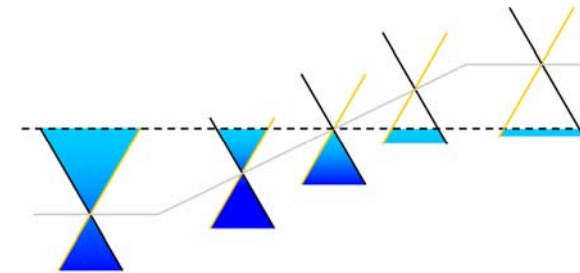


From J.R. Williams, L. DiCarlo, and C.M. Marcus, Science 317, 638

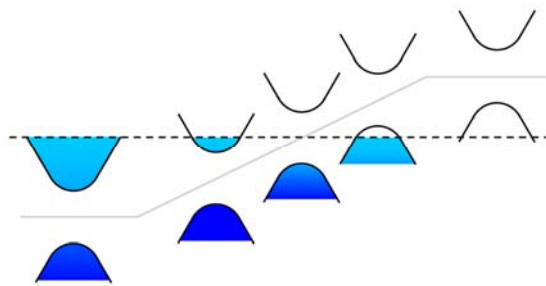
M.I. Katsnelson, K.S. Novoselov, A.K. Geim, Nature Phys. 2, 620 (2006).  
 V.V. Cheianov, V.I. Fal'ko, Phys. Rev. B 74, 041403(R) (2006)  
 V.V. Cheianov, V. Fal'ko, B. L. Altshuler, Science 315, 1252 (2007)  
 B. Huard, J.A. Sulpizio, N. Stander, K. Todd, B. Yang, and D. Goldhaber-Gordon, Phys. Rev. Lett. 98, 236803 (2007)  
 B. Özyilmaz, P. Jarillo-Herrero, D. Efetov, D. A. Abanin, L. S. Levitov, and P. Kim, Phys. Rev. Lett. 99, 166804 (2007)



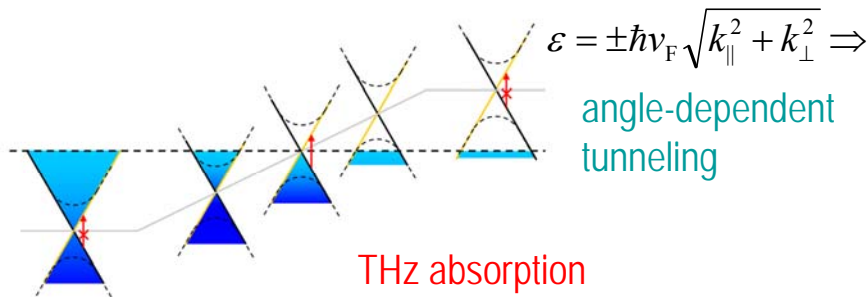
Exeter structures (A.K. Savchenko & Co)



Klein tunneling in a graphene p-n junction



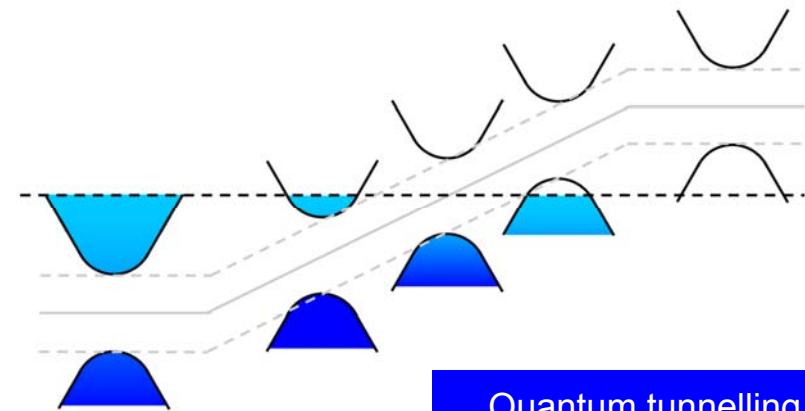
Conventional p-n junction



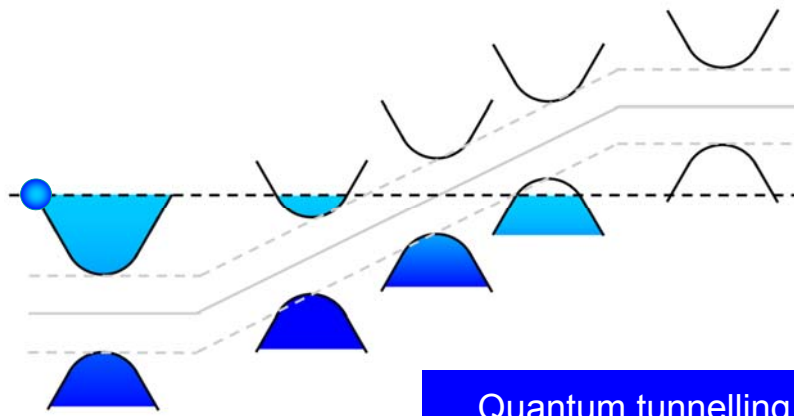
$$\varepsilon = \pm \hbar v_F \sqrt{k_{\parallel}^2 + k_{\perp}^2} \Rightarrow$$

angle-dependent tunneling

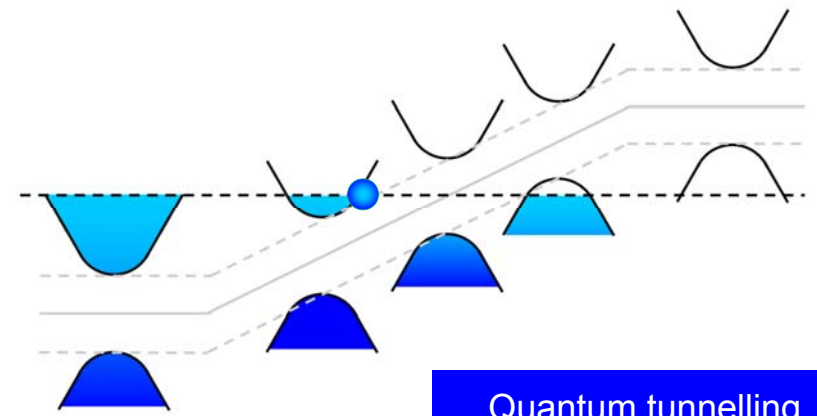
THz absorption



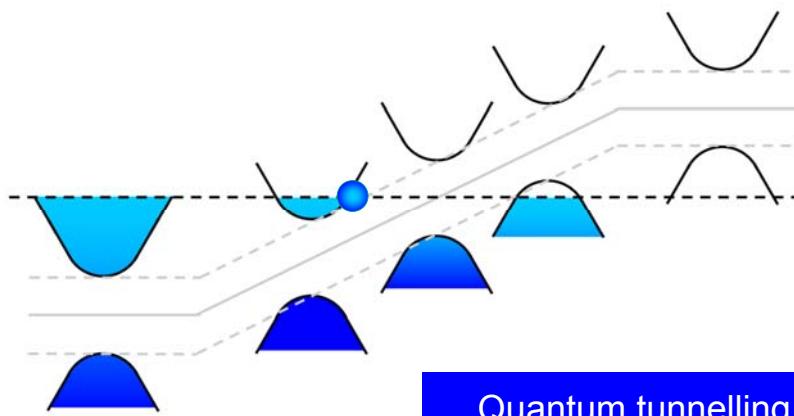
Quantum tunnelling in a conventional system



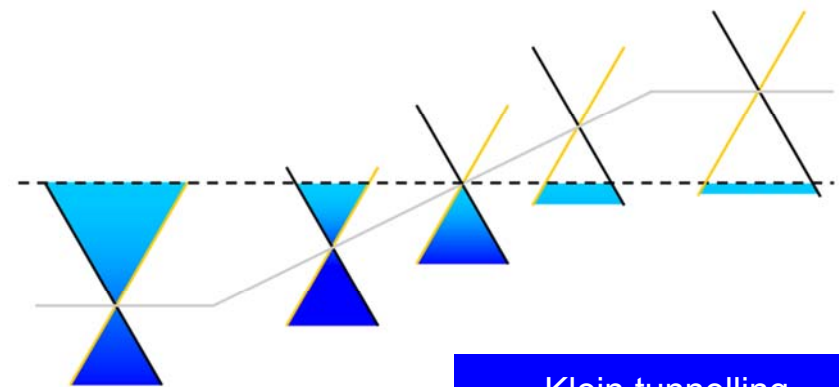
Quantum tunnelling  
in a conventional system



Quantum tunnelling  
in a conventional system



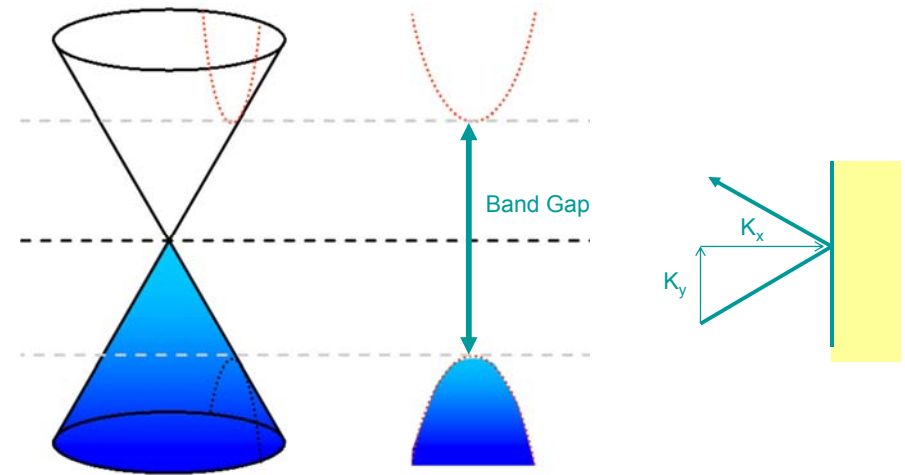
Quantum tunnelling  
in a conventional system



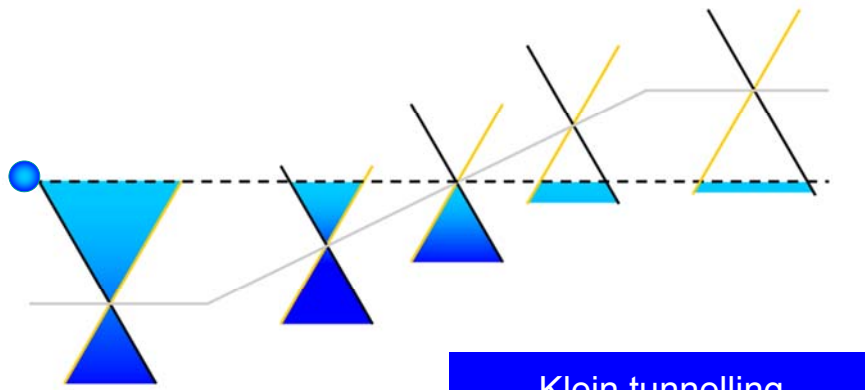
Klein tunnelling  
in a Graphene p-n junction



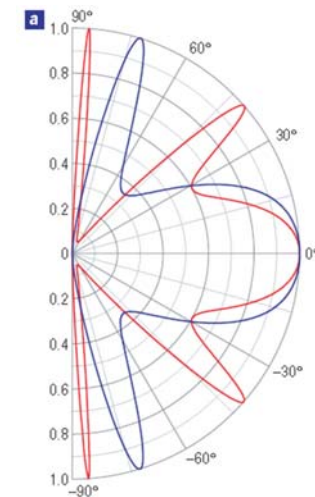
What if the incidence is not normal to a barrier?



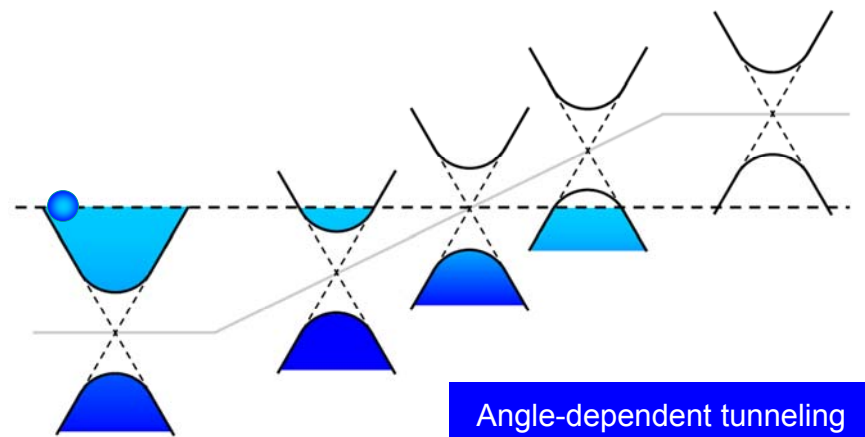
Klein tunnelling  
in a Graphene p-n junction



Tunneling probability  
in a Graphene p-n junction



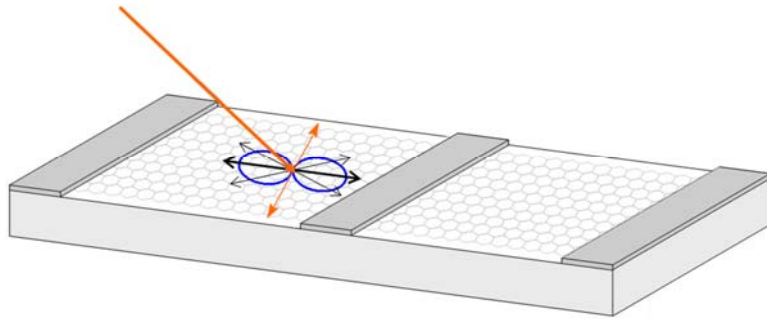
Angle-dependent tunneling  
in a Graphene p-n junction



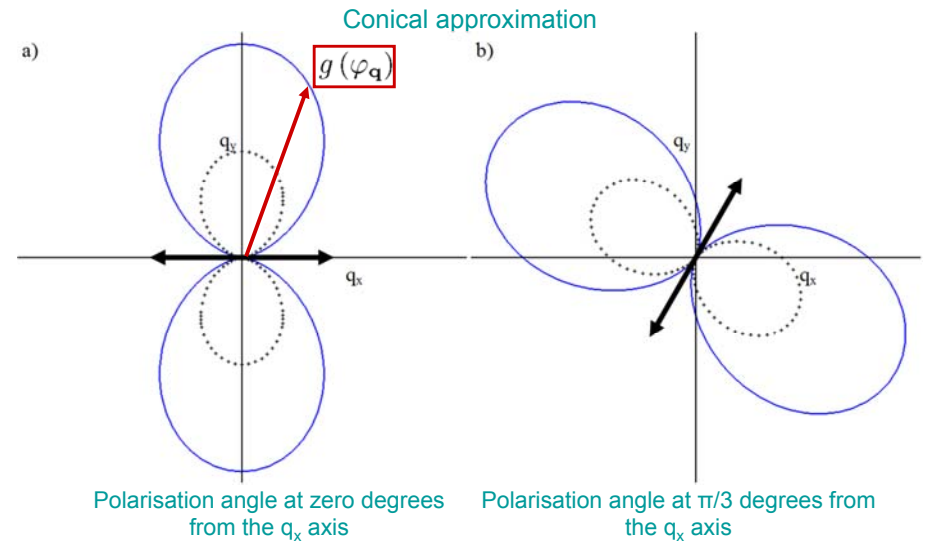
# Momentum alignment of photoexcited carriers in graphene

For  $\hbar\omega \ll \gamma_0$ ,  $|\langle C|\hat{v}|V\rangle|^2 = v_F^2 \sin^2(\varphi_p - \varphi_k) \Rightarrow$   
 $f(\mathbf{k}) \propto 1 + \alpha_0 \cos[2(\varphi_p - \varphi_k)]$  with  $\alpha_0 = -1$

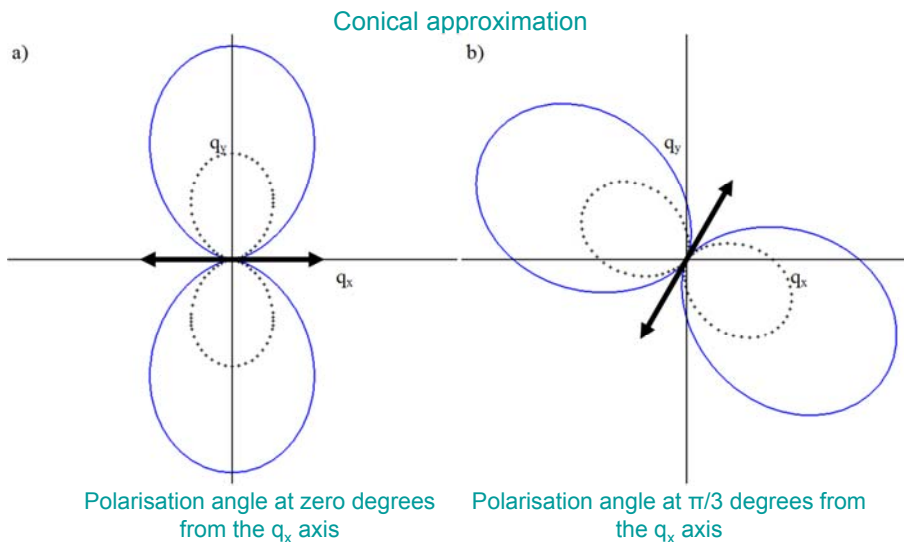
( $\mathbf{p}$  is the light polarization vector)



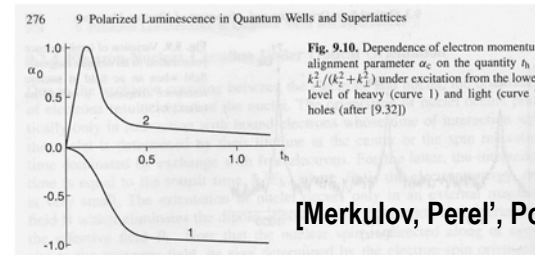
# Momentum alignment of photoexcited carriers



# Momentum alignment of photoexcited carriers



# Reminder: alignment in conventional III-V quantum wells



From E.L. Ivchenko and G.E. Pikus "Superlattices and other heterostructures", (Springer, 1997).

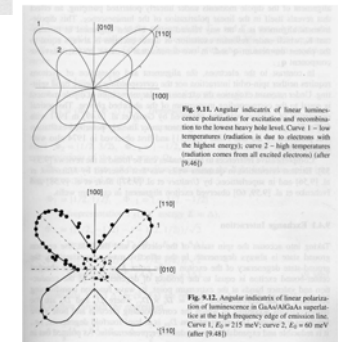
# Influence of warping

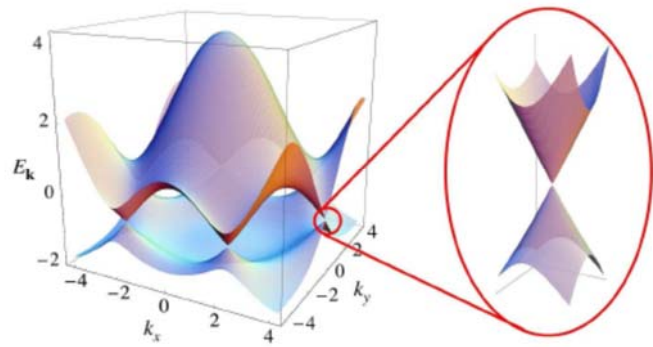
Experiment:

D.N. Mirlin & Co (1990)

Theory:

MEP (1991)



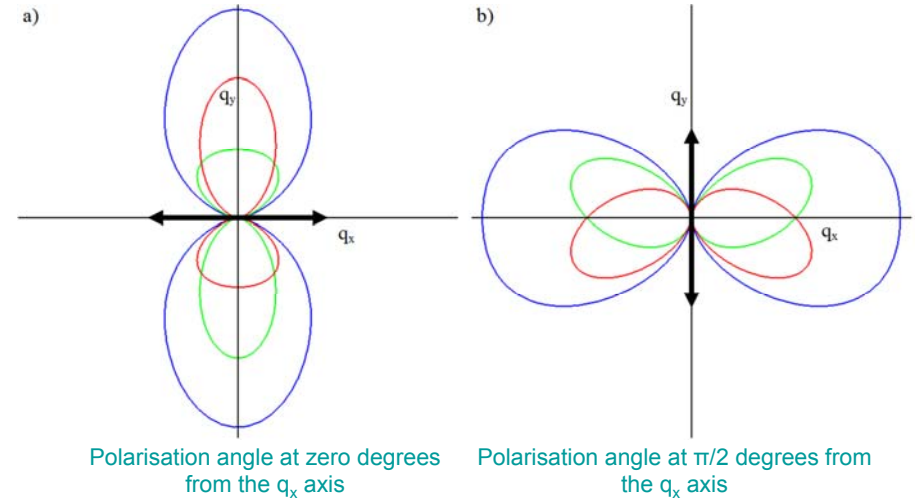


### Graphene dispersion.

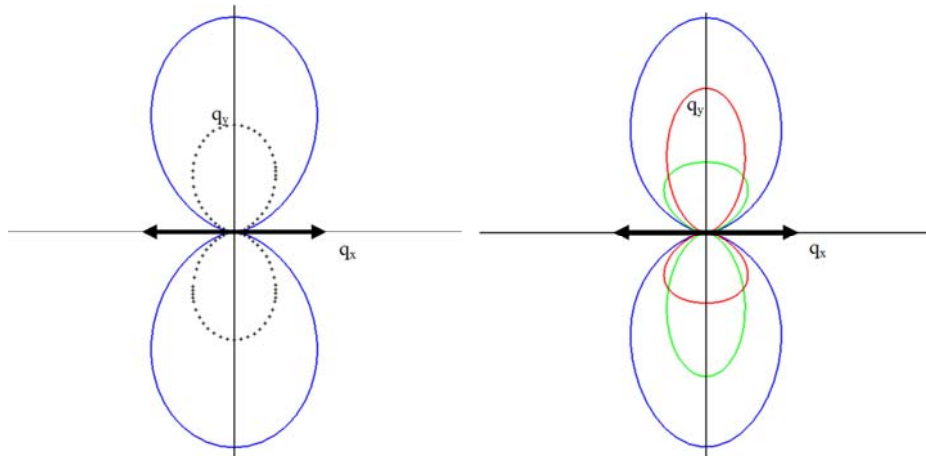
P.R. Wallace, The band theory of graphite.  
*Phys. Rev.* **71**, 622–634 (1947).

### Momentum alignment of photoexcited carriers

Trigonal warping energy regime

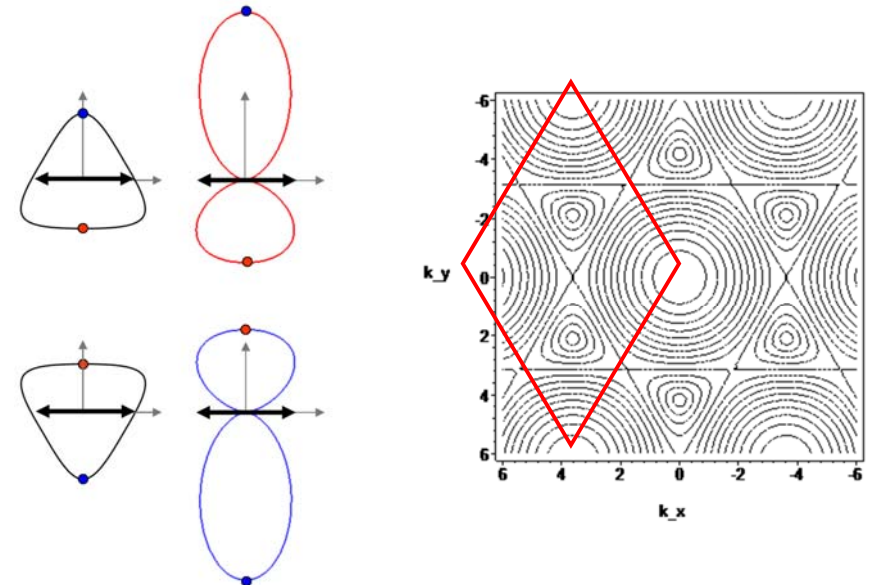


### Comparison of High and Low Energy

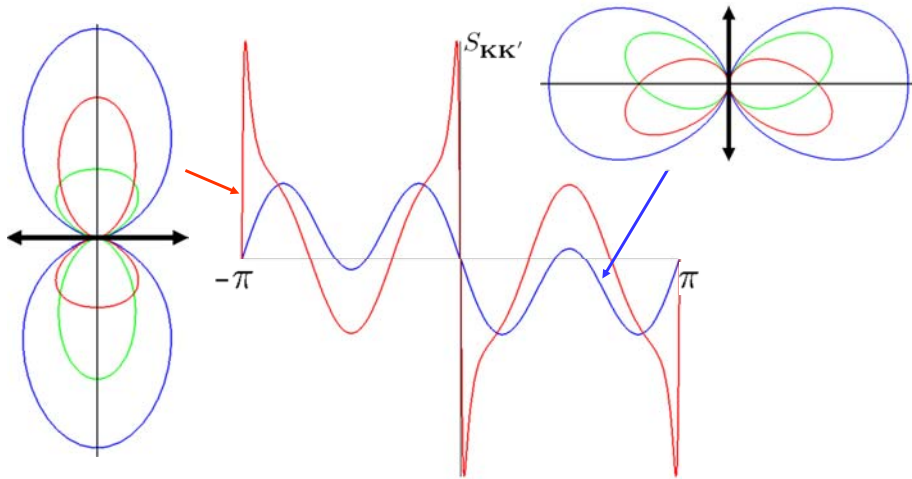


**Valley mixing is essential to preserve symmetry!**

### The effect of trigonal warping



## Optovalleytronics



$$S_{\mathbf{K}\mathbf{K}'} = \frac{F_{\mathbf{K}} - F_{\mathbf{K}'}}{F_{\mathbf{K}} + F_{\mathbf{K}'}}$$

## Summary

- We demonstrate that a quasi-metallic carbon nanotube emits radiation in the mid-infrared range, when the potential difference is applied to its ends. The typical required voltages and nanotube parameters are similar to those available in the state-of-the-art transport experiments. The maximum of the spectral density of emission is shown to have the strong voltage dependence, which is universal for all quasi-metallic carbon nanotubes in the ballistic regime.
- We also show that an electric field, which is applied normally to the axis of long-period chiral nanotubes, significantly modifies their band structure near the edge of the Brillouin zone. This results in the negative effective mass region at the energy scale below the high-energy phonon emission threshold. This effect can be used for an efficient frequency multiplication in the THz range.
- We discuss the feasibility of using the effect of magnetic field, which opens the energy gaps and allows optical transitions in armchair nanotubes, for detecting THz radiation. This effect also results in a very narrow emission line with the peak position controlled by the value of applied magnetic field.
- Graphene can be used as a polarization-sensitive THz detector with sub-wavelength spatial resolutions

Carbon-based nanostructures should be considered as promising candidates for a range of THz applications